Journal of Power Sources 188 (2009) 30–37

Contents lists available at ScienceDirect

Journal of Power Sources

journal homepage: www.elsevier.com/locate/jpowsour

Direct methanol fuel cell (DMFC) based on PVA/MMT composite polymer membranes

Chun-Chen Yang[a,*], Ying-Jeng Lee[a], Jen Ming Yang[b]

[a] Department of Chemical Engineering, Mingchi University of Technology, 84 Gungjuan Rd., Taipei Hsien 243, Taiwan, ROC
[b] Department of Chemical and Materials Engineering, Chang Gung University, Kwi-Shan, Tao-Yuan 333, Taiwan, ROC

ARTICLE INFO

Article history:
Received 13 October 2008
Received in revised form
20 November 2008
Accepted 21 November 2008
Available online 3 December 2008

Keywords:
Montmorillonite (MMT)
Composite
Polymer membrane
Direct methanol fuel cell (DMFC)

ABSTRACT

A novel composite polymer electrolyte membrane composed of a PVA polymer host and montmorillonite (MMT) ceramic fillers (2–20 wt.%), was prepared by a solution casting method. The characteristic properties of the PVA/MMT composite polymer membrane were investigated using thermal gravimetric analysis (TGA), differential scanning calorimetry (DSC), dynamic mechanical analysis (DMA), scanning electron microscopy (SEM), and micro-Raman spectroscopy, and the AC impedance method. The PVA/MMT composite polymer membrane showed good thermal and mechanical properties and high ionic conductivity. The highest ionic conductivity of the PVA/10 wt.%MMT composite polymer membrane was 0.0368 S cm^{-1} at 30 °C. The methanol permeability (P) values were 3–4 × 10^{-6} cm^2 s^{-1}, which was lower than that of Nafion 117 membrane of 5.8 × 10^{-6} cm^2 s^{-1}. It was revealed that the addition of MMT fillers into the PVA matrix could markedly improve the electrochemical properties of the PVA/MMT composite membranes; which can be accomplished by a simple blend method. The maximum peak power density of the DMFC with the PtRu anode based on Ti-mesh in a 2 M H_2SO_4 + 2 M CH_3OH solution was 6.77 mW cm^{-2} at ambient pressure and temperature. As a result, the PVA/MMT composite polymer appears to be a good candidate for the DMFC applications.

1. Introduction

The direct methanol fuel cells (DMFCs) [1–12] have recently received a lot of attention due to their high-energy density and their low emission of pollutants. The DMFCs have attracted much attention because of their usage of liquid fuel, which simplifies the problems of delivery and storage and because of their very high theoretical mass energy density (3000 Wh kg^{-1}). More importantly, liquid fuel can be used at ambient temperature and pressure, which makes the DMFC easy to use with portable 3C electronic devices [1–12]. Nafion (Du Pont), a commercially proton-conducting polymer membrane has been used in DMFCs, because this perfluorinated ionomer membrane has excellent chemical, mechanical, and electrochemical properties as well as high proton conductivity at ambient temperature and high humidity condition.

Presently, the methanol permeation not only causes a loss of fuel but also forms a mixed potential at the cathode and leads to a lower electrochemical performance (ca. at over 40% methanol loss) of the DMFC. These drawbacks have prompted research on proton-conducting polymer membranes aimed at decreasing the methanol permeability, either through the synthesis of a composite polymer electrolyte membrane, such as those of sulfonated poly(ether ether ketone) + organic-montmorillonite (SPEEK/OMMT) [1], polybenzimidazole (PBI)/montmorillonite (MMT) [2] or by modifying the Nafion polymer electrolyte membrane [3]. Thus, the solid polymer membrane for use on DMFC must have a lower value of methanol permeability and a higher proton-conducting polymer electrolyte membrane at the same time.

Recently, Pivovar et al. [4] studied poly(vinyl alcohol) polymer membrane applied on pervaporation, which has a higher affinity for water compared to alcohols. Moreover, Shao et al. [5,6] prepared the crosslinked composite membranes of Nafion and PVA. It was found that the methanol permeability was reduced by about 48%. Several studies [7–9] showed the PVA polymer membrane with the sulfonated acid to reduce methanol permeability. For the reduction of the methanol permeability through the membranes, some studies indicated the addition of inorganic fillers to improve the barrier properties of the PVA polymer, such as PVA/SiO_2 [10,11] and PVA/polyrotaxane [12]. Montmorillonite (MMT) is well-known layered silicate, which was used as the filler added into the Nafion polymer membrane [1,2]. The layered structure and high-aspect ratio of the MMT clays are expected to be able to decrease the methanol permeability owing to a winding diffusion path for methanol.

The addition of the hydrophilic MMT fillers to the PVA polymer matrix not only facilitated a reduction of the glass transition tem-

* Corresponding author. Tel.: +886 29089899; fax: +886 29041914.
E-mail address: ccyang@mail.mcut.edu.tw (C.-C. Yang).

0378-7753/$ – see front matter © 2008 Elsevier B.V. All rights reserved.
doi:10.1016/j.jpowsour.2008.11.098

perature (T_g), the crystallinity of the polymer and the increase of the amorphous phases of polymer matrix, but also increased its ionic conductivity.

As we know, when the hydrophilic MMT (clay) filler, which is a stiffer material, is added into the PVA matrix, the swelling ratio of the PVA/MMT composite polymer membrane is effectively reduced. Both the dimensional stability and the swelling ratio of the composite polymer membranes were improved.

The results indicated that the ionic conductivity, the thermal property, and the dimensional stability properties of the composite polymer membranes were enhanced when a suitable number of the MMT fillers were added into the solid polymer electrolytes (SPEs). As the MMT clays in the polymer matrix created some defects or amorphous domains at the interface between the ceramic particle and the polymer chain, an increase in the ionic conductivity of the composite polymer electrolyte occurred.

2. Experimental

2.1. Preparation of the PVA/MMT composite polymer membranes

PVA (Aldrich) and sodium-montmorillonite (Na^+-MMT) clays (Aldrich), were used without further purification. The MMT had 95 mequivalent for each 100 g of cation exchange capacity with a size of between 6 and 16 μm. Before blending, the MMT was treated with a dilute H_2SO_4 aqueous solution to convert Na^+-MMT into H^+-MMT. The H^+-MMT was washed with D.I. water several times and dried. The degree of polymerization and saponification of the PVA were 1700 and 98–99%, respectively. The PVA/MMT composite polymer membranes were prepared using a solution casting method. With the appropriate weight ratios of the PVA:MMT = 1:0.02–0.20, the PVA polymer and MMT were dissolved and dispersed in distilled water by stirring, respectively.

The resulting solution was stirred continuously until the solution mixture reached a homogeneous viscous appearance at 90 °C for 3 h. The resulting solution was poured out onto a glass plate or Petri dish. The thickness of the wet composite polymer membrane was between 0.20 and 0.40 mm. The container with the viscous PVA/MMT composite polymer solution was weighed again and then the excess water was allowed to evaporate slowly at 25 °C with a relative humidity of 30RH%. After water evaporation, the container with the composite solid polymer membrane was weighed again. The composition of the PVA/MMT composite polymer membrane was determined from the mass balance. The thickness of the composite polymer membrane was controlled in the range of 0.10–0.30 mm.

The PVA/MMT composite polymer membrane was further crosslinked by immersion in a solution of 5 wt.% glutaraldehyde (GA, 50 wt.% content in distilled water, Merck), 1.0 vol.% HCl (as a catalyst) and acetone for the crosslinking reaction at 40 °C for 12 h. The preparation methods of the PVA composite polymer electrolyte membranes by a solution casting method have been reported in detail elsewhere [13–15].

2.2. Thermal analyses

The thermal analyses of the PVA/MMT composite polymer membranes were carried out using both differential scanning calorimetry (DSC) (a PerkinElmer Pyris 7 DSC system) and thermogravimetry (TGA) (a Mettler Toledo TGA/SDT 851^e system). DSC measurements were carried out in a dry N_2 atmosphere from 25 to 250 °C with a heating rate of 10 °C min^{-1}. The glass transition temperature (T_g), the melting temperature (T_m), and the heat of fusion or enthalpy (ΔH_m) were measured from DSC thermograms. The degree of crystallinity was also determined from $X_c = (\Delta H_m/\Delta H_m^\circ) \times 100$. TGA measurements were carried out by heating from 25 to 600 °C under a N_2 atmosphere at a heating rate of 10 °C min^{-1}, with a sample about 5 mg. Dynamic mechanical analyses (DMA) were conducted using a RSA-III Instrument dynamic mechanical analyzer (TA) at a frequency of 1 Hz and oscillation amplitude of 0.15 mm. DMA measurements were carried out by heating from 25 to 150 °C under an air atmosphere at a heating rate of 5 °C min^{-1}

2.3. SEM and micro-Raman analyses

The cross-sectional view and top surface morphologies and microstructures of all PVA/MMT composite polymer membranes were investigated by a Hitachi S-2600H scanning electron microscope (SEM). The micro-Raman analysis was carried out using a confocal microscopy Raman spectroscopy system (Renishaw) including a microscope equipped with a 50× objective, and a charge-coupled device (CCD) detector. The Raman excitation source was provided by a 633 nm laser beam, which had a beam power of 10 mW which was focused on a spot of about 1 μm in diameter.

2.4. Ionic conductivity measurements

Conductivity measurements were made for the PVA/MMT composite polymer membrane by an AC impedance method. The PVA/MMT composite samples were immersed in a 2 M H_2SO_4 solution for at least 24 h before the test. The PVA/MMT composite polymer membranes were placed between SS304 stainless steel, ion-blocking electrodes, with a surface area of 1.32 cm^2, in a spring-loaded glass holder. A thermocouple was kept close to the composite polymer membrane for a temperature measurement. Each sample was equilibrated at the experimental temperature for at least 30 min before measurement. AC impedance measurements were carried out using the Autolab PGSTAT-30 Equipment (Eco Chemie B.V., Netherlands). An AC frequency range of 1 MHz to 10 Hz at an excitation signal of 5 mV was recorded. The impedance of the composite polymer membrane was recorded at a temperature range of 30–70 °C. Experimental temperatures were maintained within ±0.5 °C by a convection oven. All PVA/MMT composite polymer membranes were examined at least three times.

2.5. Methanol permeability measurements

Methanol permeability measurements were conducted by using a diffusion cell. The cell was divided into two compartments, in which one compartment was filled with D.I. water (called the B Compartment) and the other compartment filled with a 20 wt.% CH_3OH aqueous solution (called the A Compartment). Prior to the test, the PVA/MMT composite polymer membrane was hydrated in D.I. water for at least 24 h. The PVA/MMT composite polymer membrane with a surface area of 1 cm^2 was sandwiched by an O-ring and clamped tightly at between two compartments. The glass diffusion cell was continually stirred during the experiment.

The concentration of alcohol diffused from Compartments A and B across the PVA/MMT composite membrane was examined with time using density meter (Mettler Toledo, DE45). The amount of 0.25 mL was sampled from the B Compartment every 30 min. Before the permeation experiment, the calibration curve of the density vs. the methanol concentration was prepared. The calibration curve was used to calculate the methanol concentration in the permeation experiment. The methanol permeability was calculated from the slope of the straight-line plot of alcohol concentration vs. the permeation time. The methanol concentration in the B Compart-

ment as a function of time is given in Eq. (1) [16]:

$$C_B(t) = \frac{A}{V}\frac{DK}{L}C_A(t - t_o) \quad (1)$$

where C is the alcohol concentration, A and L are the polymer membrane area and thickness; D and K are the alcohol diffusivity and partition coefficient between the membrane and the solution. The product DK is the membrane permeability (P), t_o, also termed time lag, which is related to the diffusivity: $t_o = L^2/6D$.

2.6. Electrochemical measurements

The catalyst ink for the anode electrode was prepared by mixing 70 wt.% PtRu black inks (Alfa, HiSPEC 6000, PtRu black with Pt:Ru = 1:1 molar ratio), 30 wt.% PTFE binder solution (DuPont, 60 wt.% base solution), and a suitable amount of distilled water and alcohol. The resulting PtRu black mixtures were ultrasonicated for 2 h. The PtRu black inks were loaded onto the Ti-mesh by a paint-brush method to achieve a loading of PtRu black of 4.0 mg cm^{-2}. The Ti-mesh (Delker, 1 mm) current collector was cut at 1 cm × 1 cm.

The PtRu Ti-mesh anode electrode was dried in a vacuum oven at 105 °C for 3 h. The PtRu/C anode (E-TEK) with a loading of PtRu/C of 4.0 mg cm^{-2} was also used for comparison. The E-TEK cathodes with a loading of Pt/C of 4.0 mg cm^{-2} were used.

The electrochemical measurements for the DMFC were carried out in a two-electrode system. The cyclic voltammogram (CV), current density-potential (I–V), and power density curves of the DMFC comprising of the PVA/10 wt.%MMT composite polymer membrane were recorded at a scan rate of 5 mV s^{-1}, respectively. All electrochemical measurements were performed on an Autolab PGSTAT-30 electrochemical system with GPES 4.8 package software (Eco Chemie, The Netherland). The construction of the DMFC for testing has been described in detail elsewhere [15].

3. Results and discussion

3.1. Thermal analyses

Fig. 1 shows the TGA thermograph of the PVA/MMT composite polymer membrane with various MMT compositions. TGA curves of the PVA/MMT polymer films revealed three main weight loss regions, which appeared as three peaks in the DTG curves (not shown here). The first region, at a temperature of 80–100 °C ($T_{p,1}$ at 130 °C), was due to the evaporation of the physically weak and chemically strong bound H_2O; the weight loss of the membrane was about 2.5–3.7 wt.%. The second transitional region, at around 350–390 °C ($T_{p,2}$ at 390 °C), appeared to be due to the degradation of the side-chain of the PVA/MMT composite polymer membrane; the total weight loss corresponding to this stage was about 38–46 wt.%. The peak of the third stage at 435 °C ($T_{p,3}$ at 435 °C) occurred due to the cleavage C—C backbone of PVA/MMT composite polymer membrane with a total weight loss at about 90 wt.% at 600 °C, as listed in Table 1.

The degradation peaks of the crosslinked PVA/MMT composite polymer samples were less intense and shifted towards higher temperatures. It could therefore be concluded that the thermal stability was improved due to the additive effect of the MMT fillers and the chemical crosslinking reaction between the —OH group on the PVA and the —CHO group on the GA.

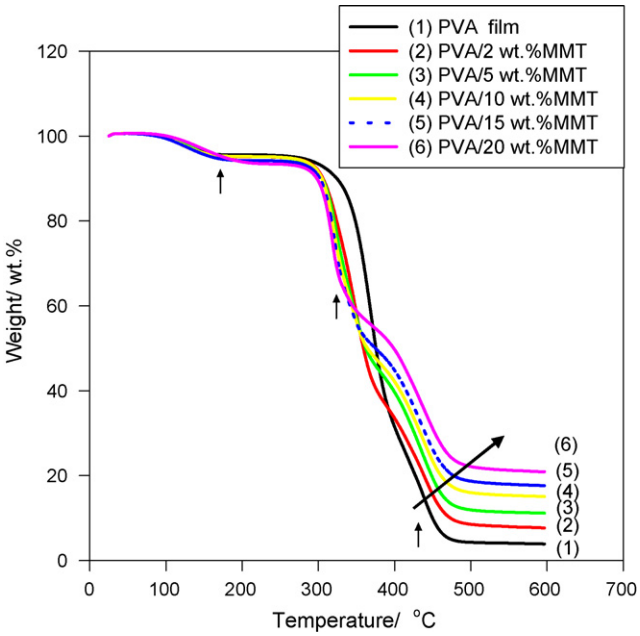

Fig. 1. TGA curve for the PVA/x%MMT composite polymer membranes.

The DSC measurements were carried out by a heating-cooling-heating cycle, so-called the H—C—H procedure. The purpose of the first heating cycle was to remove any thermal history of the PVA composite polymer membrane. The DSC (2nd heating) curves for the pure PVA polymer and the PVA/MMT composite polymer membranes with various MMT compositions (2–20 wt.%) are shown in Fig. 2. An endothermic peak was presented at 225 °C, which corresponded to the melting temperature of the pure PVA. It had been reported that the T_m of the pure PVA polymer with 98–99% hydrolysis degree was at 226 °C [9]. It was found that the melting temperature, T_m, of the PVA composite polymer membrane shifted toward lower temperature when MMT fillers were added into the PVA polymer matrix. Also, the glass transition temperature (T_g) also decreased from 81.59 to 70.82 °C. Additionally, the T_g for pure PVA film is displayed in the inset of the Fig. 2. A change of T_m of PVA/MMT composite polymer membrane indicated a change between a semi-crystalline phase and an amorphous phase.

The degree of the relative crystallinity (X_c, %) was gradually decreased from 38.35% to 9.71% when the amount of the MMT fillers varied from 0% to 20%, as listed in Table 2. It was also found that the re-crystallization peak temperature (T_c) was shifted to a lower temperature direction and the T_c peak became broaden from the DSC cooling curve (not shown here). This also indicated a change between a semi-crystalline phase and an amorphous phase.

Table 1
TGA results of weight loss of the PVA/MMT composite polymer membranes at various temperatures.

Types	Temperature					
	100 °C (%)	200 °C (%)	300 °C (%)	400 °C (%)	500 °C (%)	600 °C (%)
PVA film	0.25	4.42	6.51	67.73	95.68	96.06
PVA/2 wt.%MMT	0.51	4.86	7.98	65.97	91.39	92.29
PVA/5 wt.%MMT	0.29	5.76	8.46	59.81	87.99	88.82
PVA/10 wt.%MMT	0.44	4.78	8.20	57.38	83.91	84.91
PVA/15 wt.%MMT	0.63	5.75	9.10	54.73	81.22	82.34
PVA/20 wt.%MMT	0.60	6.08	10.28	49.84	77.75	79.08

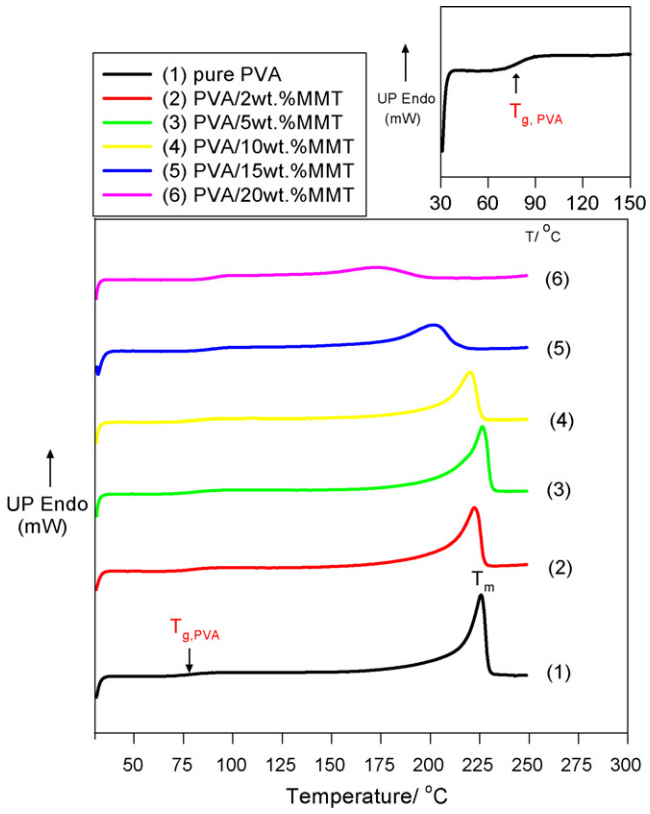

Fig. 2. DSC curves for the PVA/x%MMT composite polymer membranes (for heating cycle); the inset figure shown T_g of pure PVA.

Fig. 3(a) shows the variation of storage modulus (E') vs. temperature for the pure PVA and the PVA/MMT composite polymer membranes up to 10 wt.% MMT ceramic fillers. The storage modulus of the pure PVA ($E' = 1.36 \times 10^9$ Pa) was lower than the PVA/MMT composite polymer membranes with 5 and 10 wt.% MMT ($E' = 4.01$–5.43×10^9 Pa) at 25 °C. It was clear that the storage moduli of the PVA/MMT composite polymer membranes increased with increasing MMT filler loading (increase about three times). It also confirmed that the MMT fillers enhanced the mechanical properties of the PVA composite polymer membranes, as shown in Table 3. In particular, when the MMT filler was 20 wt.%, the stiffening effect was progressively reduced due to the agglomeration of the MMT fillers in the PVA matrix.

Fig. 3(b) shows the loss factor or tan δ vs. temperature for these PVA/MMT composite films. The glass transition temperatures (T_g) can also be taken at the peak of the tan δ curve. The results indicated that the glass transition temperatures of the pure PVA film (considered as a $T_{g,\ PVA}$) and the PVA/10 wt.%MMT SPE were 44 °C and 45 °C, respectively. The T_g values from the DMA analyses (44–45 °C)) for the PVA/MMT composite polymer membranes were lower than those from the DSC analyses (71–82 °C). Generally, the sensitivity

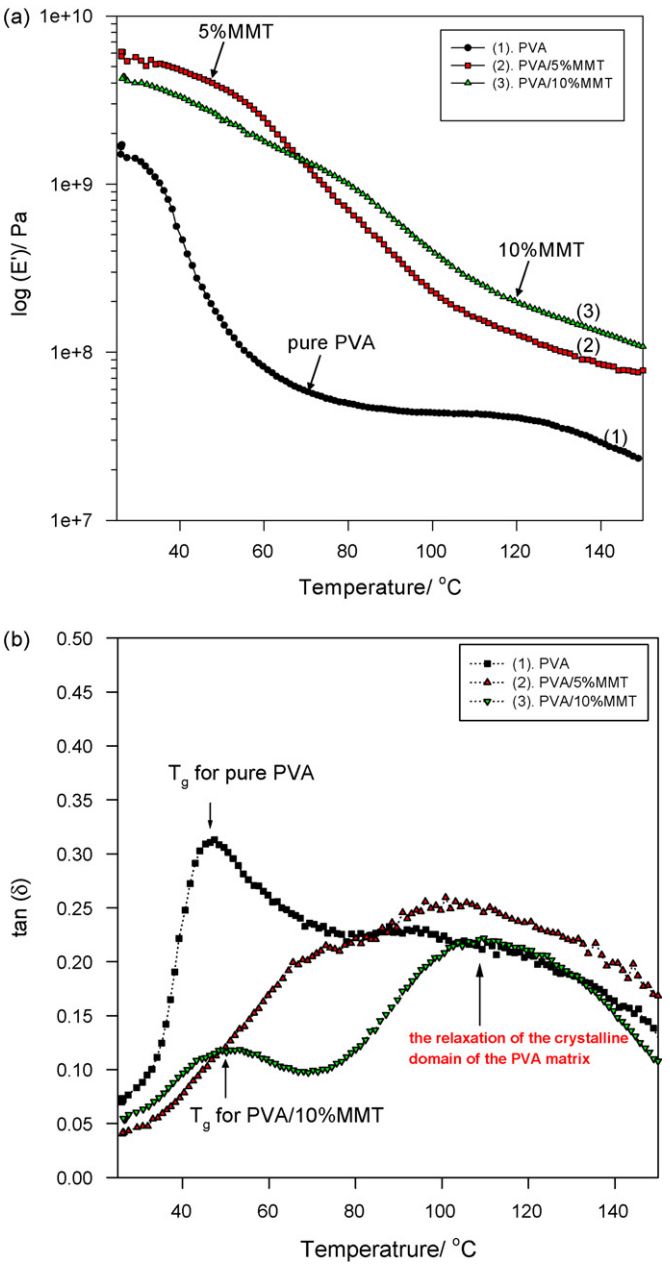

Fig. 3. (a) The storage modulus (E') vs. temperature curve and (b) the tan δ vs. temperature curves for the PVA/MMT nanocomposite SPEs.

for the measurement of a glass transition temperature by DMA is much better than that by DSC. We may be concluded that the actual T_g value for the as-prepared PVA/MMT composite polymer membrane was around 44–45 °C. It is because the lower degree of

Table 2
The DSC results of the PVA/MMT composite polymer membranes at various compositions of MMT fillers.

Types	Param.				
	T_g (°C)	ΔH_m (J g^{-1})	X_c (%)	T_m (°C)	T_c (°C)
PVA film	81.59	57.53	38.35	225.70	220.51
PVA/2 wt.%MMT	78.47	54.81	36.54	222.25	197.16
PVA/5 wt.%MMT	76.98	52.93	35.29	224.40	202.19
PVA/10 wt.%MMT	75.22	46.18	30.79	220.09	194.56
PVA/15 wt.%MMT	72.69	23.48	15.65	202.46	169.66
PVA/20 wt.%MMT	70.82	14.56	9.71	173.96	132.61

Table 3
The DMA results of the PVA/MMT composite polymer membranes at various compositions of MMT fillers.

T (°C)	Types		
	E' (Pa)		
	PVA film	PVA/5 wt.%MMT	PVA/10 wt.%MMT
30	1.36×10^9	5.43×10^9	4.01×10^9
60	7.85×10^7	2.30×10^9	1.78×10^9
100	4.36×10^7	2.23×10^8	3.88×10^8
120	4.08×10^7	1.26×10^8	1.95×10^8
150	2.32×10^7	7.77×10^7	1.08×10^8

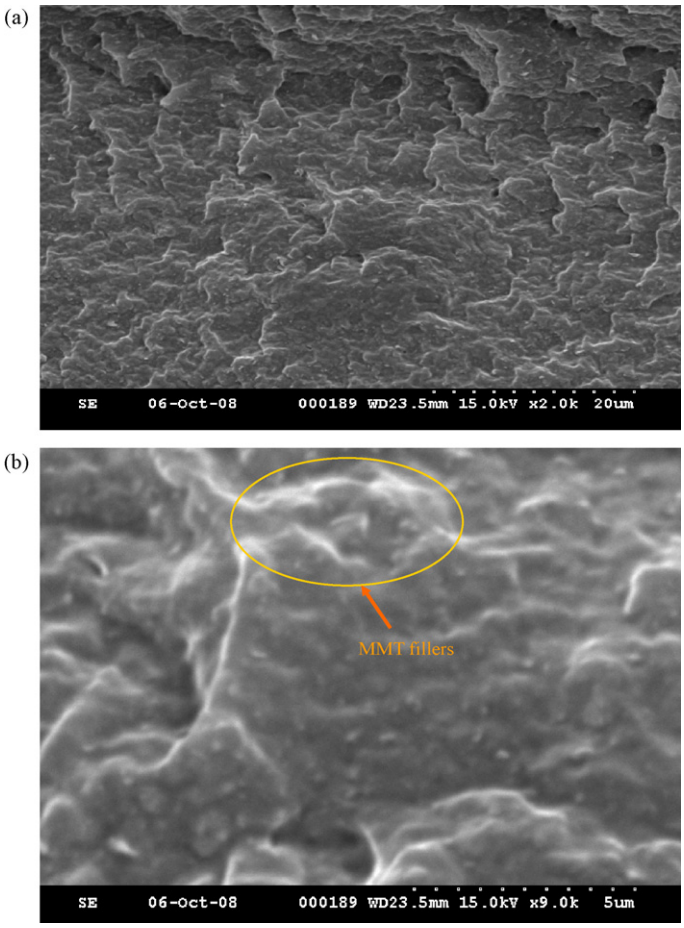

Fig. 4. SEM photographs for the PVA/10 wt.%MMT composite polymer membrane: (a) at 2 kx and (b) at 9 kx.

crystallinity of the PVA polymer host when the MMT filler is added. Apparently, it was observed that there were two distinct tan δ peaks for the PVA/10 wt.%MMT composite polymer membranes; the first tan δ peak ($T_{g,PVA}$ = 45 °C) was located between 45 and 52 °C; however, the secondary tan δ peak was found at 110 °C, the so-called the β_c relaxation; it is due to the relaxation of the crystalline domain of the PVA/MMT SPE. Interestingly, there was only one broaden tan δ peak for the PVA/5%MMTcomposite polymer membrane. It was found that the degree of crystallinity of the PVA/5 wt.%MMT SPE was higher than that of the PVA/10 wt.%MMT SPE. The DMA results are consistent with the degree of relative crystallinity (X_c, %) of the DSC analyses.

The decreasing of these tan δ peak values of PVA/MMT composite polymer membranes can be described as the incompatibility within two materials or decreasing of the degree crystallinity of the PVA/MMT SPE. The broadening of the tan δ peak may be due to the increase of the stiffness of the PVA/MMT SPEs.

3.2. SEM and micro-Raman analyses

SEM photographs of the cross-sectional views of the PVA/MMT composite polymer membrane with 10 wt.% MMT fillers at different magnifications are shown in Fig. 4(a) and (b), respectively. It was found that the MMT and the PVA polymer in the SPE were well compatible and homogenous. As seen in Fig. 4(b), magnification at 9 kx, the MMT fillers (shown as a white color) was uniformly embedded into the PVA matrix.

However, the content of the hydrophilic PVA polymer vs. the MMT ceramic filler should be controlled in order to obtain a uniform and well-dispersed composite polymer membrane. Clearly, the compatibility of the PVA polymer and MMT fillers is good when the MMT content is less than 20 wt.%. As we know, the MMT fillers (which can be used effectively as a methanol permeation barrier) in the PVA matrix can assist in reducing methanol crossover through the composite polymer membrane.

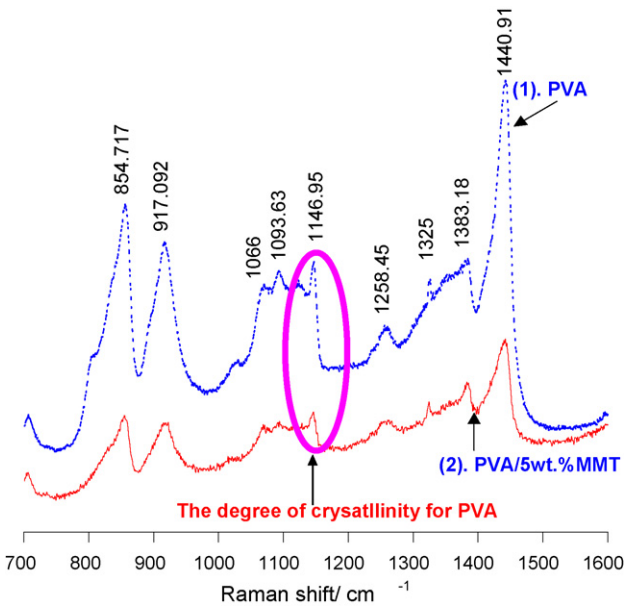

Fig. 5. Raman spectra for the pure PVA and the PVA/5%MMT composite polymer membrane.

Fig. 5 shows the micro-Raman spectra of the pure PVA film and the PVA/5 wt.%MMT composite polymer membrane, which shows some strong characteristic scattering peaks of the PVA polymer at 1440, 1145, 926, and 852 cm^{-1}, respectively. By comparison, the strong peak of the PVA polymer at 1438 cm^{-1} was due to the C—H bending and O—H bending. Moreover, the two additional vibrational peaks of the PVA polymer at 912 and 851 cm^{-1} were due to the C—C stretching. Additionally, there were several weak scattering peaks at 1145 and 1088 cm^{-1}, which were due to the C—C stretching and C—O stretching. Most importantly, it can be seen clearly that the intensities of those characteristic vibrational peaks of the PVA/5 wt.%MMT composite polymer membrane had markedly decreased; in particular, a vibrational peak at 1145 cm^{-1} is an indicator of the degree of crystallinity of the PVA polymer [17]. On the other hand, some evidence of the intensity decrease of the PVA vibrational peak at 1145 cm^{-1} has been indeed shown, which indicated an increase of amorphous domains in the PVA/MMT composite membrane.

3.3. Ionic conductivity measurements

The typical AC impedance spectra of the PVA/10 wt.%MMT composite polymer membrane by a direct blend of the PVA polymer with MMT fillers at different temperatures are shown in Fig. 6. The AC spectra were typically non-vertical spikes for stainless steel (SS) blocking electrodes, i.e., the SS |PVA/MMT SPE| SS cell. Analysis of the spectra yielded information about the properties of the PVA/MMT polymer electrolyte, such as bulk resistance, R_b. Taking into account the thickness of the composite electrolyte films, the R_b value was converted into the ionic conductivity value, σ, according to the equation: $\sigma = L/R_bA$, where L is the thickness (cm) of the PVA/MMT polymer membrane, A is the area of the blocking electrode (cm^2), and R_b is the bulk resistance (Ω) of the alkalinecomposite polymer membrane.

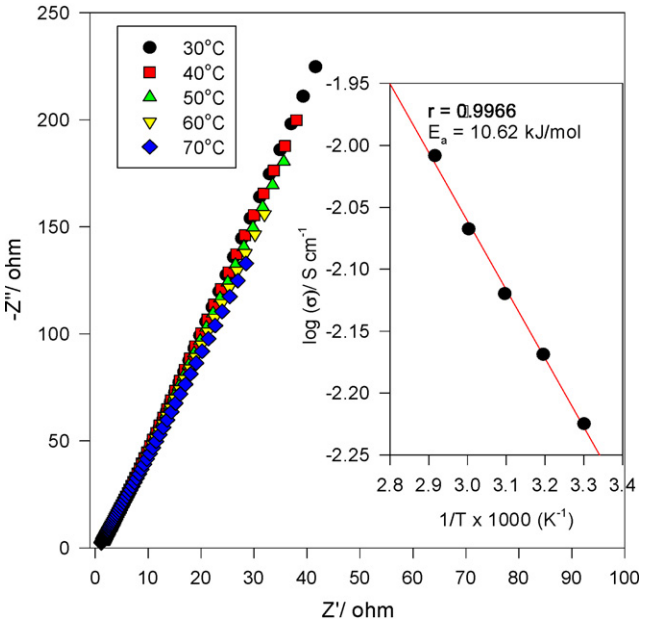

Fig. 6. Nyquist plot and Arrenhiun plot (the inset) for the acidic PVA + 10 wt.%MMT composite polymer electrolytes.

Typically, the R_b values of the PVA/MMT composite polymer membranes are of the order of 1–3 Ω and are dependent on the contents of the MMT fillers and H_2SO_4. Note that the composite polymer membrane was immersed in a 2 M H_2SO_4 solution for 24 h before measurement. Table 4 shows the ionic conductivity values of all PVA/0–20 wt.%MMT composite polymer membranes at different temperatures. As a result, the ionic conductivity value of the PVA/2 wt.%MMT composite polymer membranes was 0.0230 S cm^{-1} at 30 °C, but 0.0243 S cm^{-1} for the pure PVA membrane.

Comparatively, the ionic conductivity values of the PVA/MMT composite polymer membrane containing 5 wt.% and 10 wt.% MMT fillers were 0.0270 and 0.0368 S cm^{-1} at 30 °C, respectively. Moreover, the ionic conductivity values of the PVA/MMT composite polymer membrane comprising of 15 and 20 wt.% MMT fillers were 0.0225 and 0.0205 S cm^{-1} at 30 °C, respectively. It was found that the highest ionic conductivity value for the PVA/10 wt.%MMT composite polymer membrane was about 0.0368 S cm^{-1} at ambient temperature. Apparently, the ionic conductivity of the PVA/MMT composite polymer membranes starts to decrease when the amount of added MMT fillers was over 10 wt.%. It may be due to the formation of large aggregates or chunks (poor dispersion) in the PVA polymer matrix when too large amounts of MMT fillers were added. The formation of those aggregates is not good for the ionic transport; therefore, the ionic conductivity value gradually decreases. The $\log_{10}\sigma$ vs. $1/T$ plots, as shown in the inset of Fig. 7, obtains the activation energy (E_a) of the PVA/10 wt.%MMT composite polymer membranes, which is dependent on the contents of the MMT fillers in the PVA matrix. The E_a value of the PVA/10 wt.%MMT composite polymer membranes is of the order of 10.62 kJ mol^{-1}.

Table 4
The ionic conductivities of the PVA/MMT composite polymer membranes at various compositions of MMT fillers at different temperatures.

T (°C)	σ (S cm^{-1})					
	PVA/x%MMT composite membranes					
	0%	2%	5%	10%	15%	20%
30	0.0243	0.0230	0.0270	0.0368	0.0225	0.0205
40	0.0295	0.0260	0.0354	0.0430	0.0307	0.0231
50	0.0354	0.0293	0.0428	0.0510	0.0379	0.0271
60	0.0400	0.0301	0.0496	0.0567	0.0446	0.0293
70	0.0433	0.0319	0.0517	0.0623	0.0495	0.0278

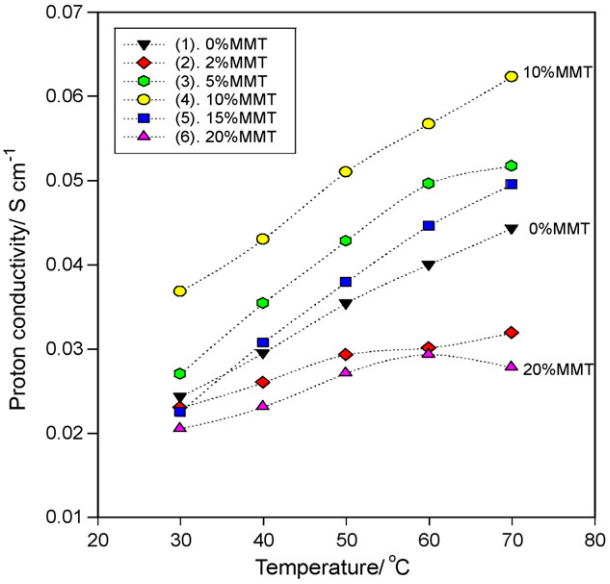

Fig. 7. The ionic conductivity vs. temperature curves for various PVA/xwt.%MMT composite polymer electrolytes.

Fig. 7 shows the ionic conductivity vs. temperature curves (at 30–70 °C) for the PVA/MMT composite polymer membranes being dipped in a 2 M H_2SO_4 solution for 24 h. It was found that the PVA/10 wt.%MMT composite polymer membrane showed the highest ionic conductivity at different temperatures.

3.4. Methanol permeability

Fig. 8 shows the typical curve of methanol concentration vs. time for the PVA/MMT composite membranes with 0–20 wt.%MMT fillers using a 20 wt.% CH_3OH aqueous solution. All values of methanol permeability tests for the PVA/MMT composite membranes were obtained from the slope of the straight line. It

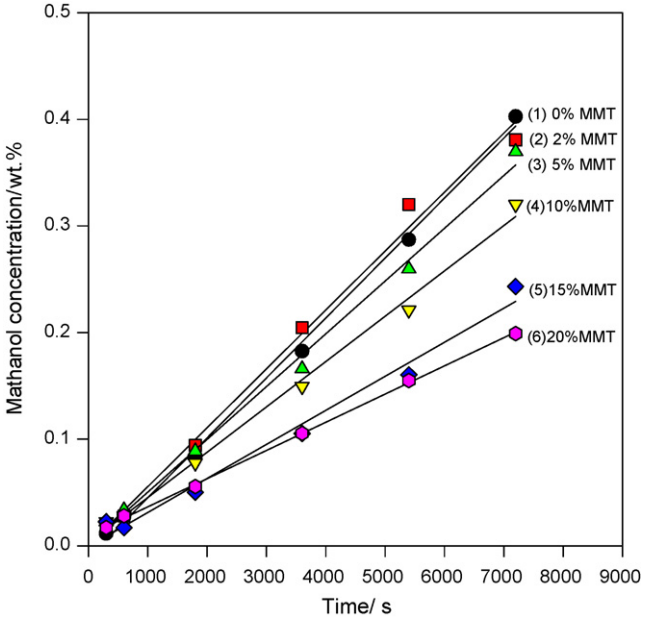

Fig. 8. The methanol concentration vs. time curve for the PVA/MMT composite polymer membranes with different amounts of the MMT fillers.

Table 5
The ionic conductivities (σ), permeability (P) and selectivity (S) values for the PVA/MMT composite polymer membranes at different compositions of MMT fillers at 25 °C.

MMT/wt.%	Para.		
	PVA/MMTcomposite membranes		
	σ (S cm^{-1})	P (cm^2 s^{-1})	$S=\sigma/P$ (S s cm^{-3})
0	0.0243	4.12×10^{-6}	5.89×10^{3}
2	0.0230	3.83×10^{-6}	6.05×10^{3}
5	0.0270	3.63×10^{-6}	7.43×10^{3}
10	0.0368	3.67×10^{-6}	1.00×10^{4}
15	0.0225	3.17×10^{-6}	7.09×10^{3}
20	0.0205	2.85×10^{-6}	7.19×10^{3}

was found that the methanol permeability (P) values of all PVA/MMT composite membranes (by a blending method) were $2.80–4\times10^{-6}$ cm^2 s^{-1}, respectively, as listed in Table 5. It is observed that the PVA/20 wt.%MMT composite membrane showed the low value of methanol permeability. The PVA/MMT composite polymer membrane with the maximum selectivity ($S=\sigma/P$) is about 1.0×10^4, which is much higher than that of Nafion 117 ca. 5.7×10^2 (our experiment result was not shown here) at 25 °C. Moreover, the permeability value of the PVA/20 wt.%MMT composite membrane ($P_{PVA/MMT}=2.85\times10^{-6}$ cm^2 s^{-1}) was lower than that of the Nafion 117 membrane ($P_{Nafion}=5.16\times10^{-6}$ cm^2 s^{-1}).

It should be noted that the PVA/MMT composite polymer membrane with lower methanol permeability could be prepared by a simple blend process. By comparison, it was found that the ionic conductivity of the PVA/10 wt.%MMT composite polymer membrane at room temperature was about 0.0368 S cm^{-1} at 30 °C and 1 atm without any humidity control, the area resistance for the PVA/10 wt.%MMT composite polymer membrane is 1.40 (Ω cm^2) at ambient temperature. However, the ionic conductivity of the Nafion 115 membrane is about 8.13×10^{-3} S cm^{-1} at 110 °C and 70%RH [18]; moreover, the Nafion 117 membrane is about 3.40×10^{-3}–0.0140 S cm^{-1} at 25 °C [19].

As the broad electrochemical stability window is important for the practical use of these membranes, a cyclic voltammogram (CV) for the SS304 |PVA/MMT SPE| SS304 cell over the range of −1.5 to 1.5 V is shown in Fig. 9. The electrochemical stability window was defined as a potential region where no appreciable faradic current flows and is limited in its cathodic and anodic parts, where the reduction and oxidation of the polymer electrolyte and H^+ ions can take place. The stability window was about 2 V for the PVA/MMT composite polymer electrolyte membranes. It was also found that the electrochemical stability window of the PVA/MMT composite membrane was better than that of the pure PVA membrane. It was found that the interfacial stability of the PVA/MMT composite polymer electrolyte (a heterogeneous interface) was much higher than that of pure PVA electrolyte (a homogeneous interface). Whereas, the interface area at between the PVA/MMT composite polymer electrolytes and the blocking electrode contains much less H_2SO_4 electrolytes, so the electrochemical window can be expanded.

Fig. 10 shows the current density-potential (I–V) and the power density-current density curves of the DMFC with the PVA/10 wt.%MMT SPE based on the PtRu/C anode (E-TEK) and the PtRu black anode (Ti-mesh), respectively, in 2 M H_2SO_4 + 2 M CH_3OH solution at room temperature. As a result, the maximum power density of 6.77 mW cm^{-2} for the DMFC based on the PtRu Ti-mesh anode was achieved at $E_{p,max}=0.316$ V with a peak current density ($i_{p,max}$) of 21.43 mA cm^{-2}. On the other hand, the maximum power density of the DMFC based on the E-TEK PtRu anode was 1.68 mW cm^{-2} at $E_{p,max}=0.179$ V with a peak current density of 9.34 mA cm^{-2} at 25 °C. Accordingly, it demonstrates here that the DMFC comprising of the PVA/10 wt.%MMT SPE with the PtRu anode (Ti-mesh) exhibits higher performance over that of the DMFC with

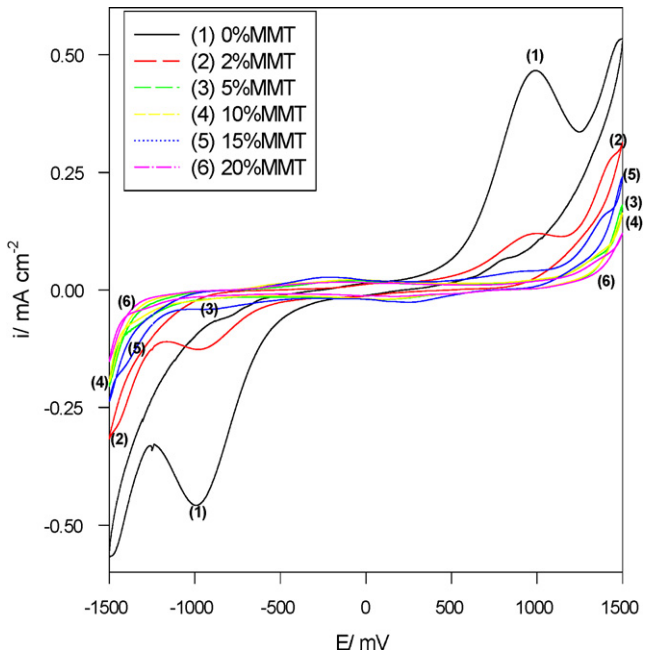

Fig. 9. The CV curve for the PVA/Xwt.%MMT composite polymer electrolytes at 5 mV s^{-1}.

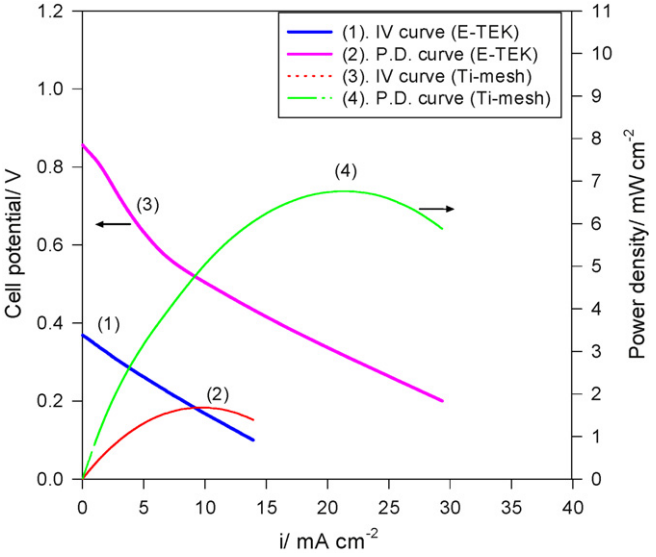

Fig. 10. The IV and P.D. curves for the DMFC using the PVA/10 wt.%MMT composite polymer membranes in a 2M H_2SO_4 + 2M CH_3OH solution at 25 °C and 1 atm.

the PtRu anode (E-TEK) at the same amount of catalyst of 4 mg cm^{-2}. More importantly, the PVA/MMT composite polymer membrane is a cheap non-perfluorosulfonated polymer membrane, as compared to the Nafion polymer membrane.

4. Conclusions

The novel composite polymer membrane based on PVA/MMT was obtained using a solution casting method. The permeability values of all PVA/MMT composite membranes were lower than those of the Nafion 117 membrane. The ionic conductivity values of the PVA/MMT composite polymer membranes were of the order of 10^{-2} S cm^{-1} at room temperature. The stability window was about 2 V for the PVA/MMT composite polymer electrolyte membranes. It demonstrated that the DMFC with the PtRu anode (with

a load of 4 mg cm^{-2}) based on Ti-mesh exhibited higher electrochemical performances than that with the PtRu/C anode based on carbon cloth. The maximum peak power density of the DMFC with the PtRu T-mesh anode in a 2 M H_2SO_4 + 2 M CH_3OH solution was 6.77 mW cm^{-2} at ambient pressure and temperature. From a practical point of view, the PVA/MMT composite polymer membranes can be prepared through a simple blending process. The PVA/MMT composite polymer membrane is a good candidate for the DMFC applications.

Acknowledgement

Financial support from the National Science Council, Taiwan (project no: NSC-96-2221-E131-009-MY2) is gratefully acknowledged.

References

[1] Z. Gaowen, Z. Zhentao, J. Membr. Sci. 261 (2005) 107.
[2] S.W. Chuang, S.L.C. Hsu, C.L. Hsu, J. Power Sources 168 (2007) 172.
[3] J.M. Thomassin, C. Pagnoulle, D. Bizzari, G. Caldarella, A. Germain, Solid State Ion. 177 (2006) 1137.
[4] B.S. Pivovar, Y. Wang, E.L. Cussler, J. Membr. Sci. 154 (1999) 155.
[5] Z.G. Shao, X. Wang, I.M. Hsing, J. Membr. Sci. 210 (2002) 147.
[6] Z.G. Shao, I.M. Hsing, Electrochem. Solid State Lett. 5 (2002) A185.
[7] J.W. Rhim, H.B. Park, C.S. Lee, J.H. Jun, D.S. Kim, Y.M. Lee, J. Membr. Sci. 238 (2004) 143.
[8] M. Kang, Y. Choi, S. Moon, J. Membr. Sci. 207 (2002) 170.
[9] W. Xu, C. Liu, X. Xue, Y. Su, Y. Lv, W. Xing, T. Lu, Solid State Ion. 171 (2004) 121.
[10] D.S. Kim, H.B. Park, J.W. Rhim, Y.M. Lee, J. Membr. Sci. 240 (2004) 37.
[11] S. Panero, P. Fiorenza, M.A. Navarra, J. Romanowska, B. Scrosati, J. Electrochem. Soc. 152 (12) (2005) A2400.
[12] J.H. Son, Y.S. Kang, J. Won, J. Membr. Sci. 281 (2006) 345.
[13] C.C. Yang, J. Power Sources 109 (2002) 22.
[14] C.C. Yang, S.J. Lin, J. Power Sources 112 (2002) 497.
[15] C.C. Yang, J. Membr. Sci. 288 (2007) 51.
[16] J. Kim, B. Kim, B. Jung, J. Membr. Sci. 207 (2002) 129.
[17] M.A. Navarra, A. Fernicola, S. Panero, A. Martinelli, A. Matic, J. Appl. Electrochem. 38 (2008) 931.
[18] Z.G. Shao, P. Joghee, I.M. Hsing, J. Membr. Sci. 229 (2004) 43.
[19] S. Haufe, U. Stimming, J. Membr. Sci. 185 (2001) 95.